



**HAL**  
open science

# A DFT study of Iodine interaction with nuclear reactor cooling system surfaces under severe accident conditions

Hao Hu, Sidi Souvi, Laurent Cantrel, Jean-François Paul

## ► To cite this version:

Hao Hu, Sidi Souvi, Laurent Cantrel, Jean-François Paul. A DFT study of Iodine interaction with nuclear reactor cooling system surfaces under severe accident conditions. *Surface Science: A Journal Devoted to the Physics and Chemistry of Interfaces*, 2021, 712, pp.121890. 10.1016/j.susc.2021.121890 . hal-03647775

**HAL Id: hal-03647775**

**<https://hal.science/hal-03647775>**

Submitted on 20 Apr 2022

**HAL** is a multi-disciplinary open access archive for the deposit and dissemination of scientific research documents, whether they are published or not. The documents may come from teaching and research institutions in France or abroad, or from public or private research centers.

L'archive ouverte pluridisciplinaire **HAL**, est destinée au dépôt et à la diffusion de documents scientifiques de niveau recherche, publiés ou non, émanant des établissements d'enseignement et de recherche français ou étrangers, des laboratoires publics ou privés.

# A DFT study of Iodine interaction with nuclear reactor cooling system surfaces under severe accident conditions

Hao HU<sup>1</sup>, Sidi SOUVI<sup>2</sup>, Laurent CANTREL<sup>2</sup>, Jean-François PAUL<sup>1\*</sup>

<sup>1</sup> Univ. Lille, CNRS, Centrale Lille, ENSCL, Univ. Artois, UMR 8181 - UCCS - Unité de Catalyse et Chimie du Solide, F-59000 Lille, France

<sup>2</sup> Institut de Radioprotection et de Sûreté Nucléaire (IRSN), PSN-RES, Cadarache, 13115 Saint-Paul-Lez-Durance Cedex, France

## Abstract:

A severe nuclear accident can lead to the release of radiotoxic iodine compounds in either aerosol form (e.g. metal iodides or iodine oxides) or gaseous form (e.g. organic iodide as CH<sub>3</sub>I or inorganic as I<sub>2</sub>) species. <sup>131</sup>I is particularly dangerous because of its possible absorption by the human body especially by the thyroid. Gaseous iodine is mainly formed in the nuclear containment building, is dispersed in the case of outside releases and may contribute in short term to long-distance contamination. Metallic iodide species are mainly formed at high temperature and partly condensed on the walls of the reactor coolant system (RCS), the rest being either deposited on the RCS or transported to the containment building. In this paper, we study theoretically, in severe accidental conditions, the adsorption of the metallic iodides on the surface of the primary circuit which is composed of Fe or Cr oxides. At high coverage, AgI and CdI<sub>2</sub> form networks on the surfaces of the RCS whereas at low coverage the molecules are isolated. This study, setting out from the stable adsorbates, investigates the chemical mechanisms leading to the iodine re-vaporization. The formation of I<sub>2(g)</sub> from adsorbed AgI or CdI<sub>2</sub> is thermodynamically and kinetically possible on over-oxidized chromium surfaces. On alternative surfaces, the co-adsorption of an oxidant, OH• issued from the steam radiolysis, is necessary to form I<sub>2(g)</sub>. This study tends to show that delayed releases of gaseous iodine are likely to happen from the deposited iodide.

**Key words:** *DFT, Iodine, Nuclear Safety, Chromium Oxide, Iron Oxide*

---

\*Corresponding author :

E-mail address : jean-francois.paul@univ-lille.fr (Jean-François PAUL)

## ***1. Introduction***

The Radiological consequences of a severe nuclear accident are mainly related to the radio toxicity of the fission products (FPs) that are, first released from degraded nuclear fuels, then transported in the reactor coolant system (RCS) and finally reach the containment building before a possible release in the environment.[1] According to their half-lives and their chemical evolutions, some isotopes are particularly dangerous.  $^{131}\text{I}$  is one of them because of the high volatility of its compounds and its important radiological consequences on human health.[2] Therefore,  $\text{I}_{2(\text{g})}$  formation should be avoided in order to limit contamination. Under severe accidental conditions, iodine can be present in either an aerosol form, either containing metal iodides ( $\text{AgI}$ ,  $\text{CsI}$ ,  $\text{CdI}_2\dots$ ) as well as iodine oxides, or gaseous form ( $\text{I}_2$  or  $\text{CH}_3\text{I}$ ).[3]

The Behaviour of metal iodide aerosols under severe accidental conditions has been long since discussed. The first study was performed by the US Nuclear Regulatory Commission in 1975.[4] The formation of these aerosols depends on accidental conditions: temperature, gas flow, the chemical affinity of iodine with the other fission products and the materials as those the control rods in the nuclear fuel are made of.[5] At high temperature, these metallic iodide species are in gas phase with likely condensation on the steel surfaces of the RCS. When the temperature cools down they form aerosols, partly deposited on the RCS surfaces whereas the rest reaches the containment where it is dissolved in the liquid phase and a small fraction is deposited by thermophoretic processes on the containment surfaces.

In the liquid phase of the containment, iodide anions issued from the soluble iodide metallic aerosols can be easily oxidized to  $\text{I}_2$  in an acidic solution.[6] This oxidation results from the gamma radiation leading to water radiolysis,  $\text{I}^-$  ions dissolved in solution can form  $\text{I}_{2(\text{g})}$  in two steps[7]: firstly,  $\text{I}^-_{(\text{aq})}$  oxidizes to  $\text{I}_{2(\text{aq})}$  under the action of oxidizing species such as  $\text{HO}^\bullet$ , then the generated  $\text{I}_{2(\text{aq})}$  evaporates to give  $\text{I}_{2(\text{g})}$ .

During the transportation through the RCS, iodine can react with silver or cadmium (the major components of the control rod alloy in PWRs[8]) to form  $\text{AgI}$  or  $\text{CdI}_2$ . [9] The formation of  $\text{I}_2$  from  $\text{AgI}$  in the liquid phase is not favorable[10] because  $\text{AgI}$  is not soluble whereas  $\text{CdI}_2$  which is soluble, forms  $\text{I}^-$  by dissolution.

Inside the reactor coolant system (RCS), aerosols onto the surface of stainless steel RCS are favoured by the important temperature gradient (thermophoresis effect). These aerosol deposits limit outside releases of fission products but an open issue is to know whether these deposits lead, to delayed releases by potential iodine remobilization.

A NEA Group of Experts[11] has detailed different ways for this potential remobilization of the fission products to occur on the primary circuit surface and inside the containment. Four mechanisms may be involved: re-suspension, re-entrainment, re-vaporization and re-volatilization. The former three phenomena may occur on the reactor coolant system (RCS) surface. The re-vaporization and resuspension of deposited fission product particles on the primary circuit surface have been considered as the main source term in the late phases of fuel degradation upon a severe nuclear accident.[12] Many studies have been made on this process.[12–16]

Thermodynamically, AgI and CdI<sub>2</sub> are two stable species in the RCS conditions.[17,18] By means of DFT calculations, H. Hijazi[19] has found that the formation of I<sub>2(g)</sub> from AgI<sub>(s)</sub> aerosols without a gaseous oxidant is impossible. However, iodinated aerosols may also condense on the walls of the primary cooling circuit consisting of 304L stainless steel tubes[5] and their reactivity changes. Experimentally, the vaporization of AgI aerosol deposits on stainless steel was studied in order to simulate the reactions likely to occur on surfaces of a RCS (reactor cooling system) in severe accident conditions<sup>20,21</sup> depending on the gas compositions. After a treatment at 750°C, under air, about half of the iodine deposited as AgI is removed as I<sub>2(g)</sub>. Under air/steam (%vol. 20/80), an important vaporization of I<sub>2(g)</sub> can be noticed and no iodine is detected on the surfaces after a thermic treatment. However, no theoretical study has been made on these processes to deepen the study of the chemical mechanism.

Cadmium could be released primarily in the case of a control rod failure.[22] In the reactor coolant system (RCS), cadmium can be expected under the form of: metal (Cd), oxide (CdO), hydroxide (CdOH) or even cadmium iodide (CdI<sub>2</sub>) in the case of a reaction with iodine compounds.[23,24] Experimentally, Gouëlle *et al.*[24] and Grégoire *et al.*[25] have found that cadmium may play an important role in the transportation of iodine in RCS. After heating metallic cadmium and caesium iodide in a crucible under three different gaseous atmospheres (different percentages of argon, steam and hydrogen) at a temperature lower than 400 °C, they observed that iodine was retained in the crucible by the possible formation of a Cd-I compound when there is no hydrogen or just a very small amount of it.<sup>24</sup> In the CHIP experimental program [17,18], the IRSN performed some tests involving Cd-Cs-I-Mo-H<sub>2</sub>O in a thermal gradient tube to study the iodine transportation through the RCS in the presence of control rod metals. Under oxidant and reducing conditions, the formation of CdI<sub>2</sub> was not experimentally evidenced but its formation is much suspected as it occurs in steam atmosphere where, with a system restricted to Cd-I-O-H, a soluble iodide aerosol is formed. Hence, it is interesting to understand the

reaction pathway of the  $\text{CdI}_2$  formation together with the possible reaction of this species with the RCS walls.

In this paper, in support of the experimental results, we perform a theoretical study of the adsorption of  $\text{AgI}$  and  $\text{CdI}_2$  on the primary circuit surface and of the mechanisms leading to their revolatilization. The 304L stainless steel is mainly composed of iron and chromium (18.17 wt. %) with small percentages of other metals (ex: Mn 1.75 wt. % etc.).[26] Using the combination of TOF-SIMS, XPS and LEIS, A.-S. Mamede *et al.*[26] have found that the nature of the oxide surface depends on both the temperature and the compositions of reactive gases. During the air oxidation, at intermediate temperature (750 °C), the surface appears as a mixture of oxides (Cr/Fe and Cr/Mn). At higher temperature (950 °C), it becomes homogeneous, the first atomic layer constituting in its majority of chromium oxide. Thus, in order to run a theoretical study on 304L stainless steel, theoretical surface model should be initially chosen. A chromium oxide surface is selected since it is the most stable at high temperature. Iron oxide, which is the base of the stainless steel appears on the surface at intermediate temperatures, therefore reactions occurring on an iron oxide surface should also be investigated. In our work, based on surface models (chromium oxide[27] and iron oxide[28]), the mechanisms of adsorption of metal iodides ( $\text{AgI}$  and  $\text{CdI}_2$ ) on stainless steel surfaces and the transformation of non-volatile iodine ( $\text{I}_{(s)}$ ) into volatile iodine ( $\text{I}_{2(g)}$ ) are theoretically studied by means of DFT calculations.

## 2. Computational Methods

### 2.1. Electronic Structure Calculations.

All calculations are performed within the Density Functional Theory (DFT) framework using the Generalized Gradient Approximation (GGA) of Perdew, Burke and Ernzerhof (PBE) [29]. The Vienna *Ab-initio* Simulation Package (VASP) [30][31] is used to solve the Kohn-Sham equations[32]. The electron wave functions are expanded on a plane-waves basis set with a cut-off energy of 600 eV. The electron-ion interactions are described within the Projector Augmented Wave (PAW) approach[33]. For the calculation related to a small cell ( $a \approx 5 \text{ \AA}$ ;  $b \approx 5 \text{ \AA}$ ;  $c = 35 \text{ \AA}$ ) and a larger one ( $a \approx 10 \text{ \AA}$ ;  $b \approx 10 \text{ \AA}$ ;  $c = 35 \text{ \AA}$ ), (5 5 1) and (3 3 1) k-point mesh were used. In the case of a transition metal, the Coulomb repulsion between electrons located in a 3d orbital is not correctly described in a spin polarized DFT treatment, therefore a DFT+U approach is used to solve the problem[34,35]. The value of U is 4 eV for Fe and Cr

with J equal to 1 eV in both cases.[27,28] The Kohn-Sham self-consistent equations are solved until the energy difference between cycles becomes lower than  $10^{-4}$  eV. The atomic positions are fully optimized until all forces applying on the atoms are smaller than 0.03 eV/ Å per atom. Different optimized structures are compared by considering their adsorption energies per adsorbed iodine molecule which are given by the following formula..

$$E_{ads} = \frac{E_{total} - E_{surface} - (E_{iodine} \times n_{iodine})}{n_{iodine}}$$

Therefore, a negative adsorption energy corresponds to an exothermic adsorption.

Moreover, the adsorption simulations are run under different coverages which can be defined by equation below:

$$r = \frac{n_{iodine \text{ adsorbed}}}{n_{Cr \text{ or Fe sites}}}$$

- $n_{iodine \text{ adsorbed}}$  : Number of adsorbed iodine molecules per unit cell.
- $n_{Cr \text{ or Fe sites}}$  : Number of Cr or Fe sites on the surface per unit cell.

To estimate the kinetic parameters of these reactions, we determined the geometries of the transition states by using the *Nudged elastic band method (NEB)* method[36–38]. As DFT calculations are performed at 0K, in order to take into account the real reactor condition (temperature and pressure), thermodynamic corrections are computed by the means of the classical statistical thermodynamic formalism[39].

## 2.2. Structural models.

S. Souvi *et al.* [27,28] have made a theoretical study on chromium and iron oxide surfaces in order to determine the most stable structure under different atmospheres ( $O_2$ ,  $H_2$  and  $H_2O$ ) at different temperatures. According to on the temperature in accidental conditions, three chromium oxide surfaces are thermodynamically stable.

At high temperature, above 900 K, the most stable is obtained by the simple cleavage of the solid and is terminated with 1 Cr and 3 O atoms, it is named **Cr<sub>2</sub>O<sub>3</sub>Cr** (*Figure 1 a*).

Below 900 K, the dissociative adsorption of  $O_2$  stabilizes the surface. In this case, one oxygen atom is adsorbed on top on the chromium atom of the surface ( $Cr_2O_3Cr$ ), called **chromyl** (*Figure 1 b*).

At ambient temperature, under steam, the surface is terminated with three OH groups the water partial pressure is lower than 3 bars. This hydrated surface is **Cr<sub>2</sub>O<sub>3</sub>Cr<sub>2</sub>(OH)<sub>3</sub>** (*Figure 1 c*).

The stability of this surface increases as the temperature decreases. At 600K,  $\text{Cr}_2\text{O}_3\text{Cr}_2(\text{OH})_3$  is stable above  $3 \cdot 10^{-3}$  bars of water partial pressure.

Above 900K, the adsorption of water and oxygen molecules is not thermodynamically stable on an iron oxide surface. Only one of  $\text{Fe}_2\text{O}_3$  structure is stable in accidental conditions inside the nuclear reactor cooling system whose surface is similar to the chromium one over large temperature and pressure. This surface is  $\text{Fe}_2\text{O}_3\text{Fe}$  (*Figure 1 d*). Over the 300–900 K range, the outermost iron atoms are almost fully hydroxylated and the chemistry of the surface is dominated by hydrogen bonds. The adsorption of molecules is unfavourable, consequently it is not discussed in this paper.

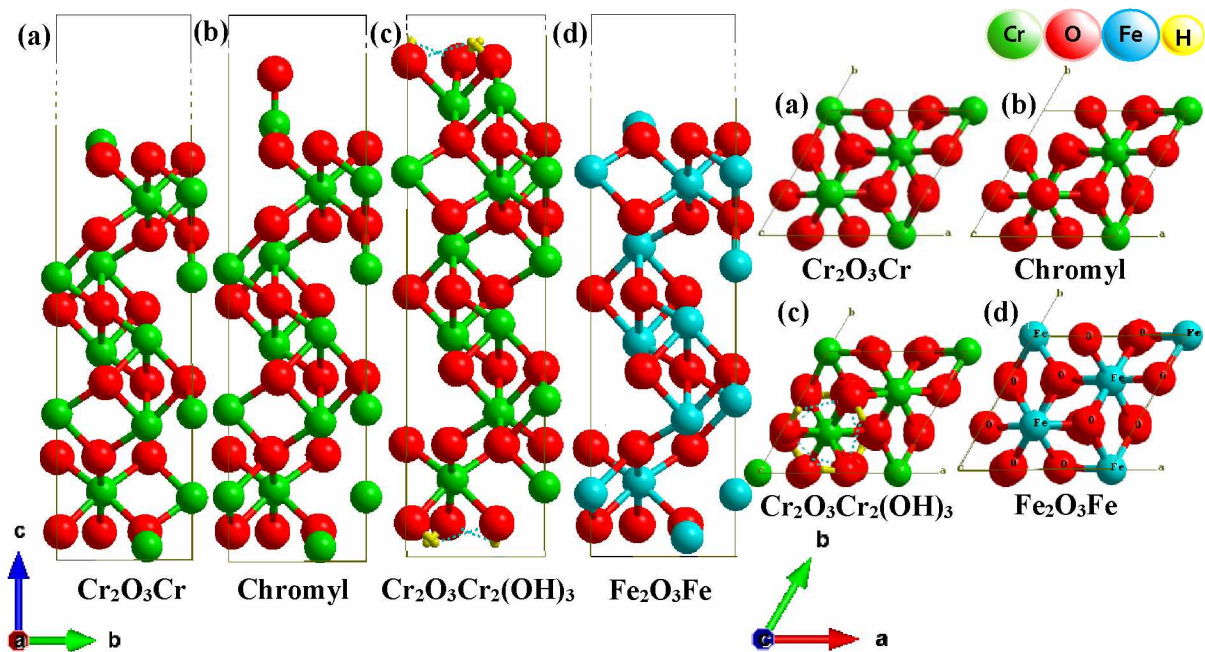


**Figure 1.** Theoretical models for the chromium oxide and iron oxide surfaces under different pressures, temperatures and atmospheres.[27,28] from left to right side and top views of surfaces. (a)  $\text{Cr}_2\text{O}_3\text{Cr}$  (neutral chromium oxide), (b) **Chromyl** (oxidized chromium oxide), (c)  $\text{Cr}_2\text{O}_3\text{Cr}_2(\text{OH})_3$  (hydrated chromium oxide), (d)  $\text{Fe}_2\text{O}_3\text{Fe}$  (neutral iron oxide). Chromium: green. Iron: blue. Oxygen: red. Hydrogen: yellow.

### 3. Results and Discussions

#### 3.1. Adsorption of AgI and CdI<sub>2</sub> on chromium oxide and iron oxide surfaces.

In order to calculate the adsorption energies of metal iodides (AgI and CdI<sub>2</sub>) on a stainless steel surface, AgI or CdI<sub>2</sub> molecules are adsorbed on four different surfaces consisting of :  $\text{Cr}_2\text{O}_3\text{Cr}$

(neutral chromium oxide), **chromyl** (oxidized chromium oxide), **Cr<sub>2</sub>O<sub>3</sub>Cr<sub>2</sub>(OH)<sub>3</sub>** (hydrated chromium oxide) and **Fe<sub>2</sub>O<sub>3</sub>Fe** (neutral iron oxide)[27,28]. Their adsorption energies per adsorbed molecule appear in **Table 1**. The most stable geometries on these different surfaces are presented in **Table 4**. All calculations are made in function of the AgI coverage. All configuration in **Figure 1**, are represented in 1×1 cellule. In view of the size of cellules, there is only one possible adsorption site, corresponding to a 100% coverage. Calculations have been made in larger cells (2x2) to study coverage of 50 and 25%. It is worth noticing that the stable structures are molecular adsorption, except on the chromyl surface with an AgI coverage below 25%.

**Table 1.** Adsorption energy per AgI or CdI<sub>2</sub> adsorbed for different coverage percentage of AgI or CdI<sub>2</sub> on chromium oxide and iron oxide surfaces

Model.	AgI Coverage			CdI <sub>2</sub> Coverage		
	25%	50%	100%	25%	50%	100%
Cr Cr <sub>2</sub> O <sub>3</sub> Cr	-1.51 eV	-1.82 eV*	-1.81 eV*	-1.40 eV	-1.40 eV	-0.52 eV*
Cr Chromyl	-1.41 eV	-1.42 eV*	-1.60 eV*	-0.36 eV	-0.80 eV	-0.56 eV*
Cr Cr <sub>2</sub> O <sub>3</sub> Cr <sub>2</sub> (OH) <sub>3</sub>	-1.21 eV	-1.51 eV*	-1.47 eV*	-0.04 eV	-0.22 eV*	-0.42 eV*
Fe Fe <sub>2</sub> O <sub>3</sub> Fe	-1.93 eV	-2.15 eV*	-2.23 eV*	-2.50 eV	-2.35 eV	-0.64 eV*

\* AgI or CdI<sub>2</sub> forms a chain/2D network. The energy can be decomposed in the energy of the chain/network formation and the interaction energy between the chain and the surface

### 3.1.1. Adsorption of AgI on chromium oxide and iron oxide surfaces.

On a **Cr<sub>2</sub>O<sub>3</sub>Cr** (neutral chromium oxide), the most stable structure of AgI is a η<sub>3</sub> geometry (Ag-OOO) where the silver atom is located in an oxygen trifold hollow site of the surface. At low coverage (i.e. 25%), the adsorbed AgI molecule is just bonded to the surface. Its adsorption energy is -1.51 eV. When the coverage increases (50% and 100%), bonds are formed between the adsorbed AgI molecules, which creates a chain on the surface. The adsorption energy increases slightly (E<sub>ads</sub>= -1.81 eV) because of the chain formation, which can decompose, per adsorbed AgI, into the chain formation from molecular AgI (E<sub>form</sub>= -1.11 eV) and in chain adsorption on the surface (E<sub>ads</sub>(chain) = -0.70 eV). Within the case when there are isolated AgI molecules on the surface, the adsorption energy per AgI is -1.50 eV, it is 0.30 eV less stable than in the case when AgI forms a chain over the surface.

On the **chromyl** surface (oxidized chromium oxide), at a low coverage (25%, **Erreur ! Source du renvoi introuvable.a**), AgI is dissociated on the surface. The silver atom is located in bridging position between terminal oxygen atoms while the iodine atom is directly bonded to a

terminal oxygen atom. Adsorption is weaker than on neutral surface ( $E_{\text{ads}} = -1.41$  eV). When the coverage increases and reaches 50%, AgI forms a chain with a similar adsorption energy (**Erreur ! Source du renvoi introuvable.**,  $E_{\text{ads}} = -1.42$  eV). The adsorption energy per AgI is  $-1.19$  eV when AgI molecules are isolated on the surface. The chain adsorption on the chromyl surface is weaker than on the bare surface ( $E_{\text{ads}}(\text{chain}) = -0.30$  eV per AgI). When the AgI coverage is 100% on the chromyl surface, AgI molecules form a 2D network composed of six membered rings. As the result of the formation of bonds between silver atoms and terminal oxygen atoms, this network is in epitaxy with the surface (**Erreur ! Source du renvoi introuvable.**). Its adsorption energy per AgI is  $E_{\text{ads}} = -1.63$  eV ( $E_{\text{form}}(\text{network}) = -1.44$  eV and  $E_{\text{ads}}(\text{network}) = -0.19$  eV). This type of cyclic structure appears in the solid silver iodide.

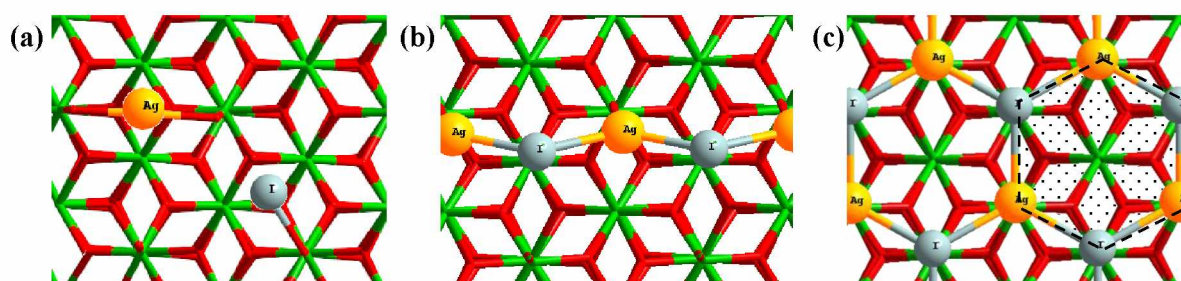


**Figure 2.** Top view of the adsorption of AgI at 25% (a) 50% (b) 100% (c) coverages on a chromyl surface. Chromium: green. Oxygen: red. Silver: yellow. Iodine: grey.

On a  $\text{Cr}_2\text{O}_3\text{Cr}_2(\text{OH})_3$  (hydrated chromium oxide surface), at a 25% coverage, AgI is isolated on the surface with a Ag atom located in a trifold oxygen hollow site ( $\eta_3$  geometry (Ag-OOO)). In comparison with the other chromium oxide surfaces, the adsorption is less favourable ( $E_{\text{ads}} = -1.21$  eV). When the coverage increases to 50%, the AgI molecules form a chain. The distance between the chain and the surface is large, between 2.5 to 3.5 Å. The interaction between the chain and the surface is weak ( $E_{\text{ads}}(\text{chain}) = -0.40$  eV and  $E_{\text{ads}} = -1.51$  eV, per AgI). Half of the Ag atoms are still located on the hollow position on the surface, whereas the others have moved away from the hollow position and do not form any bond with the surface. The AgI molecules do not form many real bonds with the surface. When the coverage reaches 100%, AgI forms a network with six membered rings as on the chromyl surface. However the interaction between the AgI network and the surface is very weak ( $E_{\text{ads}}(\text{network}) = -0.04$  eV per adsorbed AgI) without any bond between the surface and the AgI network.

The geometries of  $\text{Fe}_2\text{O}_3\text{Fe}$  and  $\text{Cr}_2\text{O}_3\text{Cr}$  surfaces are almost similar. As a consequence, the AgI adsorption geometries are similar. On a  $\text{Fe}_2\text{O}_3\text{Fe}$  (neutral iron oxide), at a low coverage (25%), silver atom is located in trifold hollow site of the surface and remains isolated ( $E_{\text{ads}} = -$

1.93 eV). At higher coverage, the adsorbed AgI also forms a chain. The chain adsorption energies are respectively -1.03 eV and -1.10 eV per AgI adsorbed in the case of 50% and 100% respective coverages ( corresponding to total adsorption energies  $E_{ads} = -2.15$  eV and -2.23 eV). The adsorption energies of isolated moieties equal to -2.09 eV in the case of a 50% coverage is slightly less favourable. On the whole, the adsorption interaction, whose energy ranges from -1.93 eV to -2.23 eV per adsorbed AgI, according to the coverage, is slightly higher than in the case of a neutral chromium oxide ( $Cr_2O_3Cr$ ) whose energy ranges from -1.51 eV to -1.80 eV.

The influence of the coverage over the different surface on the Ag-I distance is given in **Table 2**. The influence of the coverage on the Ag-O distance is given in Supporting Information **Table S1**, but is not significative. Over  $Cr_2O_3Cr$  and  $Fe_2O_3Fe$  surfaces, the evolution of bond Ag-I distance is similar. The Ag-I distance increases in the case of a high coverage surface (50% and 100%) as the molecules form a chain over these surfaces.. As the configuration of AgI on **chromyl** and  $Cr_2O_3Cr_2(OH)_3$  surfaces depends on the coverage (For a 25% coverage, AgI is isolated over the surface; for a 50% coverage AgI is in chain a configuration and for a 100 coverage, , AgI forms a 2D network), the distance increase with the coverage.

**Table 2.** Ag-I bond length in function of AgI coverages over chromium oxide and iron oxide surfaces.

Model	Ag-I bond length function of AgI coverage (Å)		
	25%	50%	100%
$Cr_2O_3Cr$	2.666	2.824	2.787
		2.840	2.853
Chromyl	4.547 (dissociation)	2.689	2.858
		2.739	2.903
			2.940
$Cr_2O_3Cr_2(OH)_3$	2.654	2.700	2.857
		2.702	2.860
			2.870
$Fe_2O_3Fe$	2.685	2.887	2.891
		2.923	2.940

In conclusion, at high coverage, AgI tends to form on the surface a chain or ring structure rather than isolated moieties. AgI adsorbs in likewise with similar adsorption energy on neutral chromium oxide ( $Cr_2O_3Cr$ ) and neutral iron oxide ( $Fe_2O_3Fe$ ). From a thermodynamic point of view, adsorption is more stable on neutral surfaces than on modified (oxidized or hydrated) surfaces. It can also be noticed that the adsorption is more favourable on an iron oxide surface is than on chromium oxide surface.

### 3.1.2. Adsorption of $CdI_2$ on chromium oxide and iron oxide surfaces.

On a  $\text{Cr}_2\text{O}_3\text{Cr}$  surface,  $\text{CdI}_2$  is also adsorbed in an oxygen trifold hollow site, which leads to the formation of three Cd-O bonds. At 25% and 50% coverages,  $\text{CdI}_2$  is isolated on the surface with an adsorption energy of -1.40 eV per adsorbed  $\text{CdI}_2$  (**Figure 3** a and b). When the coverage reaches 100%,  $\text{CdI}_2$  forms a cycle that has no contact with the surface (**Figure 3** c); the adsorption energy corresponds to condensation energy of  $\text{CdI}_2$  with a very small interaction between the  $\text{CdI}_2$  network and the surface ( $E_{\text{ads}} = -0.52$  eV with  $E_{\text{ads}}(\text{network}) = -0.10$  eV).

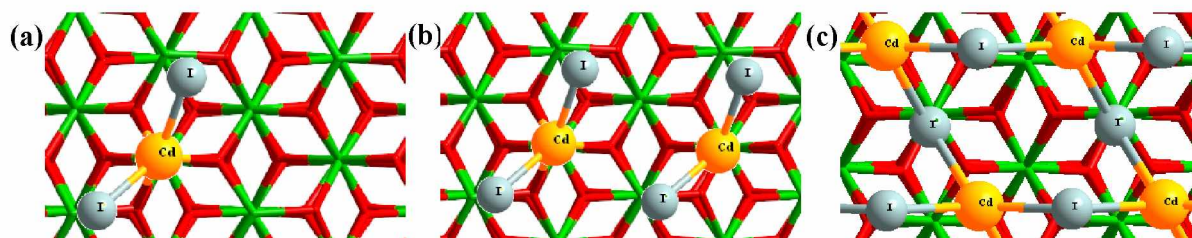


**Figure 3.** Top view of the most stable structure for  $\text{CdI}_2$  adsorbed on  $\text{Cr}_2\text{O}_3\text{Cr}$  surface at 25% (a) 50% (b) and 100% (c) coverage. Chromium: green. Oxygen: red. Cadmium: yellow. Iodine: grey.

On a **chromyl** surface, at a 25% coverage, Cd is adsorbed between two terminal oxygen atoms of the surface with an adsorption energy lower than that of the other surfaces ( $E_{\text{ads}} = -0.36$  eV). It is located in the centre of a tetrahedral structure that is formed by the two terminal oxygen atoms of the surface and two iodine atoms. When the coverage reaches 50%, the  $\text{CdI}_2$  group is adsorbed in top position on the terminal oxygen of the surface and forms a dimer (**Figure 4b**). The adsorption energy is -0.80 eV per  $\text{CdI}_2$ . When the surface is totally covered by  $\text{CdI}_2$  (**Figure 4c**),  $\text{CdI}_2$  forms a chain that forms no covalent bonds with the surface; the formation energy of this chain equal to -0.56 eV per  $\text{CdI}_2$  ( $E_{\text{ads}}(\text{chain}) = -0.36$  eV).

On a  $\text{Cr}_2\text{O}_3\text{Cr}_2(\text{OH})_3$  (hydrated chromium oxide) surface), in the case of a 25% coverage,  $\text{CdI}_2$  has no contact with the surface, hence its adsorption energy is almost zero ( $E_{\text{ads}} = -0.04$  eV). When coverage reaches 50%,  $\text{CdI}_2$  forms a chain but has still almost no contact with the surface. The adsorption energy is  $E_{\text{ads}} = -0.22$  eV with almost no interaction between the chain and the surface ( $E_{\text{ads}}(\text{chain}) = -0.04$  eV). When coverage reaches 100%,  $\text{CdI}_2$  forms a 2D network on the surface as on a  $\text{Cr}_2\text{O}_3\text{Cr}$  surface, it has no contact with the surface ( $E_{\text{ads}}(\text{network}) = 0.00$  eV). Consequently, the  $\text{CdI}_2$  adsorption is not favoured on the hydrated surface.

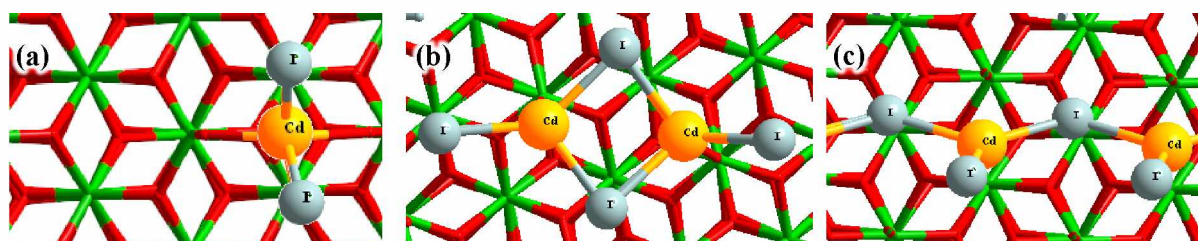


**Figure 4.** Top view of the most stable structure for CdI<sub>2</sub> adsorbed on the chromyl surface at 25 % (a) 50% (b) and 100% (c) coverages. Chromium: green. Oxygen: red. Cadmium: yellow. Iodine: grey.

On a **Fe<sub>2</sub>O<sub>3</sub>Fe** (neutral iron oxide) surface: the adsorbed CdI<sub>2</sub> reacts in the same manner as on the neutral chromium oxide surface and forms a  $\eta_3$  structure (Cd-OOO). CdI<sub>2</sub> is isolated in the case of 25% and 50% coverages where the adsorption energies are -2.50 eV and -2.35 eV respectively; adsorption is significantly more exothermic than on Cr<sub>2</sub>O<sub>3</sub>Cr (-1.40 eV). In the case of 100% coverage, CdI<sub>2</sub> also forms a 2D network above the surface. ( $E_{\text{ads}} = -0.64$  eV and  $E_{\text{ads}}(\text{network}) = -0.22$  eV).

**Table 3** shows the evolution of the Cd-I and Cd-O bonds lengths in function of the CdI<sub>2</sub> coverage on the surfaces

As regards the **Cr<sub>2</sub>O<sub>3</sub>Cr** surface, in the case of for 25% and 50% coverages, the CdI<sub>2</sub> molecules are isolated on the surface, the Cd-I and Cd-O bond lengths are similar. When CdI<sub>2</sub> forms a network over the totally covered surface, the Cd-I bond length increases slightly and there is no Cd-O bond.

As regards the **Chromyl** surface, the configurations of CdI<sub>2</sub> vary in function of the CdI<sub>2</sub> coverage: at a 25% coverage, CdI<sub>2</sub> is isolated over the surface between two terminal oxygen atoms. At 50% coverage CdI<sub>2</sub> is in a dimer configuration on top of two terminals oxygen atoms. When the surface is totally covered by CdI<sub>2</sub>, CdI<sub>2</sub> forms a network having no real bond with the surface.

As regard the **Cr<sub>2</sub>O<sub>3</sub>Cr<sub>2</sub>(OH)<sub>3</sub>** surfaces, the Cd-I and Cd-O bond lengths vary also with the coverage: At a 25% coverage, CdI<sub>2</sub> is isolated over the surface; at a 50% coverage, CdI<sub>2</sub> is in a chain configuration and when the surface totally covered by CdI<sub>2</sub>, CdI<sub>2</sub> forms a 2D network. All these configurations do not form bond with the surface which is totally hydrated. Both Cd-I and Cd-O bond lengths increase with the coverage.

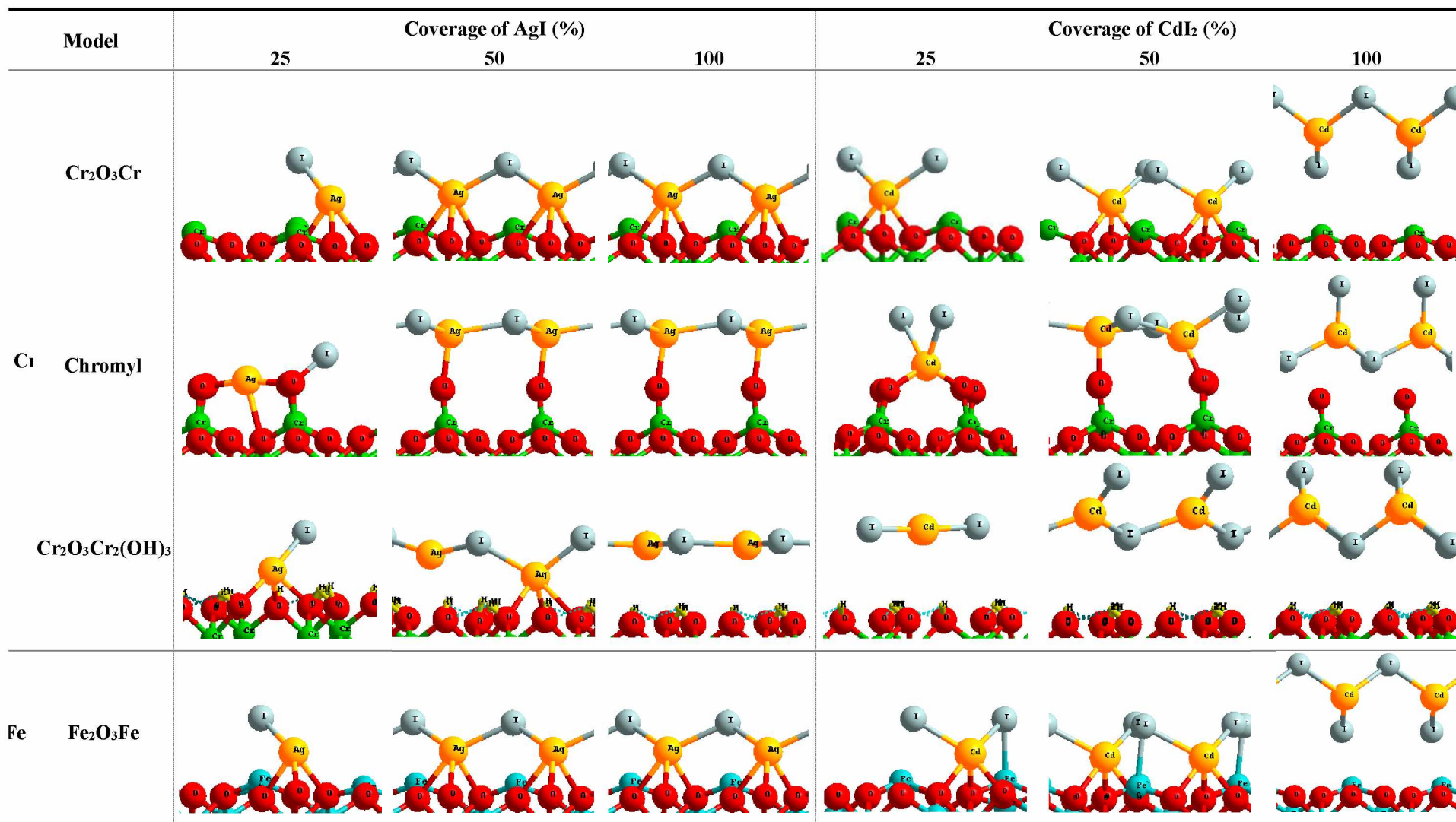
As regard the **Fe<sub>2</sub>O<sub>3</sub>Fe** surface, the evolution of the bonds is similar to that over the **Cr<sub>2</sub>O<sub>3</sub>Cr** surface. The Only difference is that at a 50% coverage, one I atom in the CdI<sub>2</sub> molecule forms a I-O bond with the surface, so the one Cd-I bond length increases in each CdI<sub>2</sub> molecule.

**Table 3.** Bond lengths of Cd-I and Cd-O in function of CdI<sub>2</sub> coverages over chromium oxide and iron oxide surfaces.

Model	Bond	Bonds lengths in function of CdI <sub>2</sub> coverage (Å)					
		25%		50%		100%	
Cr <sub>2</sub> O <sub>3</sub> Cr	Cd-I	2.802		2.791	2.829	2.952	2.960
		2.805		2.840	2.916	2.972	2.984
	Cd-O	2.332		2.366	2.391	5.419	5.667
		2.430		2.416	2.424	5.749	
		2.443		2.460	2.616	(no bond)	
Chromyl	Cd-I	2.819		2.761	2.815	2.652	2.844
		2.820		2.828	2.834	2.953	
	Cd-O	2.181	2.398	2.179	2.286	3.740	(no bond)
Cr <sub>2</sub> O <sub>3</sub> Cr <sub>2</sub> OH <sub>3</sub>	Cd-I	2.608		2.640	2.643	2.944	2.950
		2.609		2.878	2.880	2.984	2.989
	Cd-O	3.919	4.261	4.749	4.761	5.247	5.545
		4.291		4.793	4.808	5.899	
		(no bond)		4.997	5.009	(no bond)	
Fe <sub>2</sub> O <sub>3</sub> Fe	Cd-I	2.831		2.818	2.835	2.938	2.968
		2.838		3.015	3.019	2.986	3.078
	Cd-O	2.259		2.362	2.370	5.035	5.363
		2.394		2.371	2.392	5.465	
		2.395		2.389	2.389	(no bond)	

In conclusion, at high coverage, CdI<sub>2</sub> forms a 2D network on the surface, with almost no interaction with the surfaces. On the iron oxide surface, adsorption of CdI<sub>2</sub> is slightly more favourable than on the chromium oxide surface in which case, adsorptions on a neutral surface are much more favourable than on modified (oxidized or hydrated) surfaces.

**Table 4.** Adsorption of AgI and CdI<sub>2</sub> on chromium oxide and iron oxide surfaces in function of coverage. Chromium: green. Iron: bleu oxygen: red. Silver/Cadmium: yellow. Iodine: grey.



### 3.2. Reactivity.

The quantification of potential gaseous releases During a nuclear accident is a key point, the formation of  $I_{2(g)}$ ,  $AgI_{(g)}$  or  $CdI_{2(g)}$  from adsorbed species on surfaces is investigated. In **Table 5**, the formation energies of  $I_{2(g)}$ ,  $AgI_{(g)}$  or  $CdI_{2(g)}$  and sublimation energy of  $AgI_{(g)}$  or  $CdI_{2(g)}$  on the most interesting three surface models are reported. All calculations are based on most stable structures with different AgI or CdI<sub>2</sub> coverages. The configurations for the relaxation of the surface after I<sub>2</sub> gas desorption (Surface-n Ag and Surface-n Cd) in function of AgI or CdI<sub>2</sub> coverage are presented in **Table S3**.

**Table 5.** Formation energy of  $I_{2(g)}$  and sublimation energy of  $AgI_{(g)}$  or  $CdI_{2(g)}$  from different surface models with AgI or CdI<sub>2</sub> adsorbed.

	Reaction	Coverage of AgI or CdI <sub>2</sub>	Model	$\Delta$ Energy (eV)
<b>Formation I<sub>2</sub></b>	1 Surface-AgI → Surface-Ag + ½I <sub>2(g)</sub>	25%	Cr <sub>2</sub> O <sub>3</sub> Cr	2.36
			Chromyl	0.20
			Fe <sub>2</sub> O <sub>3</sub> Fe	2.13
	2 Surface-2AgI → Surface-2Ag + I <sub>2(g)</sub>	50%	Cr <sub>2</sub> O <sub>3</sub> Cr	5.41
			Chromyl	0.71
	<b>Sublimation AgI or CdI<sub>2</sub></b>	3 Surface-4AgI → Surface-4Ag + 2I <sub>2(g)</sub>	100%	Fe <sub>2</sub> O <sub>3</sub> Fe
Cr <sub>2</sub> O <sub>3</sub> Cr				10.63
Chromyl				3.09
4 Surface-CdI <sub>2</sub> → Surface-Cd + I <sub>2(g)</sub>		25%	Fe <sub>2</sub> O <sub>3</sub> Fe	9.06
			Cr <sub>2</sub> O <sub>3</sub> Cr	3.38
5 Surface-2CdI <sub>2</sub> → Surface-2Cd + 2I <sub>2(g)</sub>		50%	Chromyl	-0.08
	Fe <sub>2</sub> O <sub>3</sub> Fe		4.28	
	Cr <sub>2</sub> O <sub>3</sub> Cr		6.77	
6 Surface-4CdI <sub>2</sub> → Surface-4Cd + 4I <sub>2(g)</sub>	100%	Chromyl	1.35	
		Fe <sub>2</sub> O <sub>3</sub> Fe	8.27	
		Cr <sub>2</sub> O <sub>3</sub> Cr	10.47	
<b>Sublimation AgI or CdI<sub>2</sub></b>	7 Surface-AgI → Surface + AgI <sub>(g)</sub>	25%	Chromyl	4.35
			Fe <sub>2</sub> O <sub>3</sub> Fe	8.79
			Cr <sub>2</sub> O <sub>3</sub> Cr	1.51
	8 Surface-2AgI → Surface + 2AgI <sub>(g)</sub>	50%	Chromyl	1.29
			Fe <sub>2</sub> O <sub>3</sub> Fe	1.93
	9 Surface-4AgI → Surface + 4AgI <sub>(g)</sub>	100%	Cr <sub>2</sub> O <sub>3</sub> Cr	3.65
Chromyl			2.84	
Fe <sub>2</sub> O <sub>3</sub> Fe			4.31	
10 Surface-CdI <sub>2</sub> → Surface + CdI <sub>2(g)</sub>	25%	Cr <sub>2</sub> O <sub>3</sub> Cr	7.26	
		Chromyl	6.50	
		Fe <sub>2</sub> O <sub>3</sub> Fe	8.87	
			Cr <sub>2</sub> O <sub>3</sub> Cr	1.40
			Chromyl	0.36
			Fe <sub>2</sub> O <sub>3</sub> Fe	2.50

			Cr <sub>2</sub> O <sub>3</sub> Cr	2.81
11	Surface-2CdI <sub>2</sub> → Surface + 2CdI <sub>2(g)</sub>	50%	Chromyl	1.61
			Fe <sub>2</sub> O <sub>3</sub> Fe	4.70
12	Surface-4CdI <sub>2</sub> → Surface + 4CdI <sub>2(g)</sub>	100%	Cr <sub>2</sub> O <sub>3</sub> Cr	2.09
			Chromyl	2.25
			Fe <sub>2</sub> O <sub>3</sub> Fe	2.61

Comparing comparison between the formation energies with AgI adsorbed on the three different surfaces indicates that the most favourable reaction is the formation of I<sub>2(g)</sub> on **chromyl** surface (oxidized chromium oxide) surface. At a 25% coverage (**Table 5, Reaction 1**), the formation of I<sub>2(g)</sub> is slightly endothermic ( $\Delta E = 0.20$  eV). The formation of I<sub>2(g)</sub> from a chromyl surface at a 50% coverage is more endothermic ( $\Delta E = 0.71$  eV) since it will induces a greater reduction of the surface. With CdI<sub>2</sub> adsorbed, it can be noticed that the formation of I<sub>2(g)</sub> is thermodynamically favoured on a **chromyl** surface at low coverage (25%) (**Table 5, Reaction 4**,  $\Delta E = -0.08$  eV). However, because of the formation of dimers or chains at higher coverage, the interaction with the surface is reduced, the formation of I<sub>2(g)</sub> on a chromyl surface becomes endothermic ( $\Delta E = 1.35$  eV at a 50% coverage and  $\Delta E = 4.04$  eV for 100%). In this case, the sublimation of CdI<sub>2</sub> is more favourable ( $\Delta E = 1.61$  eV at a 50% coverage and  $\Delta E = 1.36$  eV for 100%).

DFT calculations are performed at 0 K whereas the temperature inside the reactor coolant system (RCS) may vary between about 450 K and 1500 K. Thus, in order to take into account the conditions of the reactor, thermodynamic corrections are made. As regards for I<sub>2(g)</sub>, AgI<sub>(g)</sub> and CdI<sub>2(g)</sub>, the thermodynamic corrections are all the more significant at high temperature, since silver, cadmium and iodine atoms are heavy. Consequently, at high temperature, there may exist a competition between the formations of I<sub>2(g)</sub> and sublimation of AgI<sub>(g)</sub> or CdI<sub>2(g)</sub>.

### 3.2.1. Formation of I<sub>2(g)</sub> on oxide surfaces with AgI adsorbed.

After thermodynamic correction terms for I<sub>2(g)</sub> and AgI<sub>(g)</sub> have been taken into account, the Gibbs free energies of I<sub>2(g)</sub> formation and AgI<sub>(g)</sub> sublimation on three most interesting surfaces are calculated and shown in **Figure 5**. It can be noticed that the formation of I<sub>2(g)</sub> is impossible on the Cr<sub>2</sub>O<sub>3</sub>Cr and Fe<sub>2</sub>O<sub>3</sub>Fe surfaces as the sublimation of AgI<sub>(g)</sub> (red lines) occurs at a temperature lower than that of the formation of I<sub>2(g)</sub> (black lines) (**Figure 5a** and **c**). Furthermore, the sublimation of AgI<sub>(g)</sub> is thermodynamically favoured only when  $\Delta_r G < 0$ . Consequently, as regards the Cr<sub>2</sub>O<sub>3</sub>Cr surface, the sublimation of AgI<sub>(g)</sub> occurs at about 560 K for a 25% coverage, at about 655 K for 50 % and 100 % coverages. Besides, as regards the Fe<sub>2</sub>O<sub>3</sub>Fe surface, the sublimation temperatures for AgI<sub>(g)</sub> adsorbed the surface with coverages

equal to 25 %, 50 % and 100 % are 700 K, 765 K and 795 K. On the chromyl surface (**Figure 5b**), it can be noticed that, at low temperature, the formation of  $I_{2(g)}$  (black curve) is always more favourable than the sublimation of  $AgI_{(g)}$  (red curve).  $I_{2(g)}$  can be formed almost spontaneously (at 75 K) at a 25% coverage while the  $AgI_{(g)}$  sublimation is thermodynamically possible only above 550 K and becomes more favourable than the  $I_{2(g)}$  formation above 930 K. When the coverage increases to 50%, the formation of  $I_{2(g)}$  can occur between 305 K and 780 K. When the temperature is higher,  $AgI_{(g)}$  sublimates. When the surface is totally covered by AgI (100%), the formation of  $I_{2(g)}$  occurs within a very small ranges of temperature (595-640 K). At higher temperature, the AgI adsorbed on the surface sublimates.

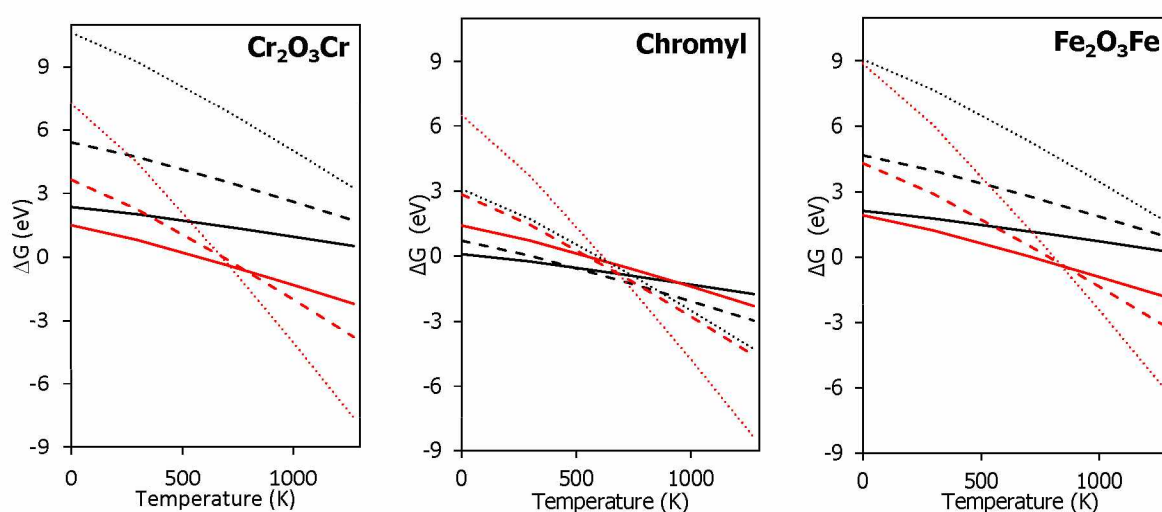


**Figure 5.** Gibbs free energies for the  $I_{2(g)}$  formation (black lines) and the  $AgI_{(g)}$  sublimation (red lines) on the three surfaces ( $Cr_2O_3Cr$ , Chromyl,  $Fe_2O_3Fe$ ) at a AgI coverage of 25% (solid line), 50% (dashed line) and 100 % (dotted line) in function of the temperature varying from 0 to 1273 K..

Since the formation of  $I_{2(g)}$  on chromyl surface can occur, the reaction pathway is discussed. At a 25% coverage, the AgI geometry on chromyl surface, which is the most stable is dissociated (**Table 4**) then the reaction mechanism of forming  $I_{2(g)}$  from  $AgI_{(g)}$  is be simple (**Figure 6**). First, AgI is adsorbed on the surface, Ag being on top of the terminal oxygen (**A**→**B**). Then AgI occupies a bridging position between two terminal oxygen (**C**) before undergoing an exothermic dissociation (**B**→**C**→**D**;  $\Delta E = -0.35$  eV). Finally,  $I_{2(g)}$  can be formed from two I generated by the dissociation of two AgI molecules (**D**→**E**;  $\Delta E = 0.20$  eV). Intermediate **C** is associated with a very low minimum, the activation energy of the **B**→**C** reaction is very close to the reaction energy (0.13 eV). In the transition state between **C** and **D** (**TS1**) whose activation energy is 0.77 eV Ag-I bond length increases (**C**:  $d_{Ag-I} = 2.62$  Å; **TS1**:  $d_{Ag-I} = 3.97$  Å and **D**:  $d_{Ag-I} = 4.55$  Å) and the iodine atom move from the top position on the Ag atom towards one of the

terminal oxygen atoms of the chromyl surface. In order to determine the transition state between state **D** and **E** (liberation of  $I_{2(g)}$ ), a larger surface (double size) containing two iodine atoms is used. The activation energy of this step is 0.64 eV ( $TS_2$ ) and the bond length between two iodine atoms decreases. One iodine atom is still located on top of one terminal oxygen atom of the surface whereas the second iodide moves from top position to form a I-I bond. An  $I_{2(g)}$  molecule is formed and can be released from the surface. Hence, with several steps slightly endothermic and low activation energies ( $\Delta E_{\text{activation}} < 0.80$  eV), this reaction can occur rapidly inside the reactor coolant system when the temperature is high. In conclusion,  $I_{2(g)}$  can be liberated into the air when the AgI coverage is less or equal to 25% on chromyl surface.

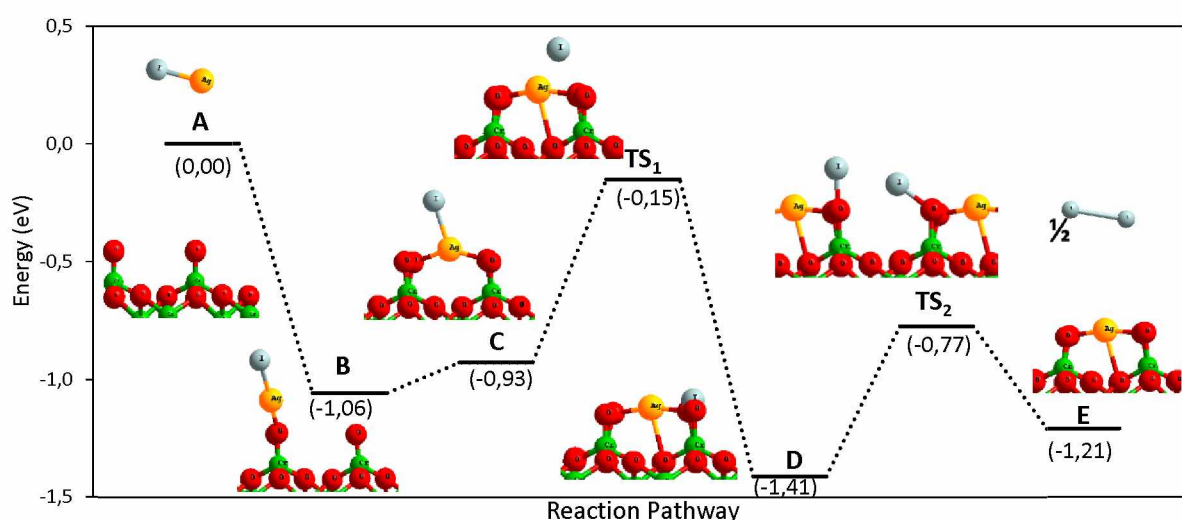


**Figure 6.** Energy diagram for the formation of  $I_2$  on a chromyl surface with 25% of AgI coverage. Chromium: green. Oxygen: red. Silver: yellow. Iodine: grey.

As shown in **Figure 5b**, at a 50% coverage, the  $I_{2(g)}$  formation can also occur. The reaction pathway is shown in **Figure 7**. At such a coverage, AgI forms a very stable chain on the surface (**B**) ( $\Delta E = -2.84$  eV). After the compression and the distortion of this chain (**C**), two AgI molecules are separated and go between two terminal oxygen atoms of the chromyl surface (**D**). finally, the distance between two iodine atoms decreases until  $I_2$  is formed and is released from the surface (**E**). All the previous steps are endothermic. In the **B**  $\rightarrow$  **C** step, the AgI chain is distorted, and forms small segments containing two AgI molecules ( $TS_1$  and **C**). The transition state ( $TS_1$ ) has an activation energy of 0.52 eV. In the **C**  $\rightarrow$  **D** step, the bond between two AgI fragments is broken and the iodine atoms move to place between two terminal oxygen atoms of the chromyl surface ( $TS_2$ ) with an activation energy higher than that of the first step (0.83 eV). In the **D**  $\rightarrow$  **E** step in which  $I_{2(g)}$  is formed, the distance between two iodine atoms decreases (**D**: 3.25 Å;  $TS_3$ : 3.08 Å and **E**: 2.66 Å). The activation energy of this step is even higher than

that of the previous ones (1.14 eV). In Comparison with the reaction at a lower AgI coverage, the activation energy increases and the reaction becomes endothermic.

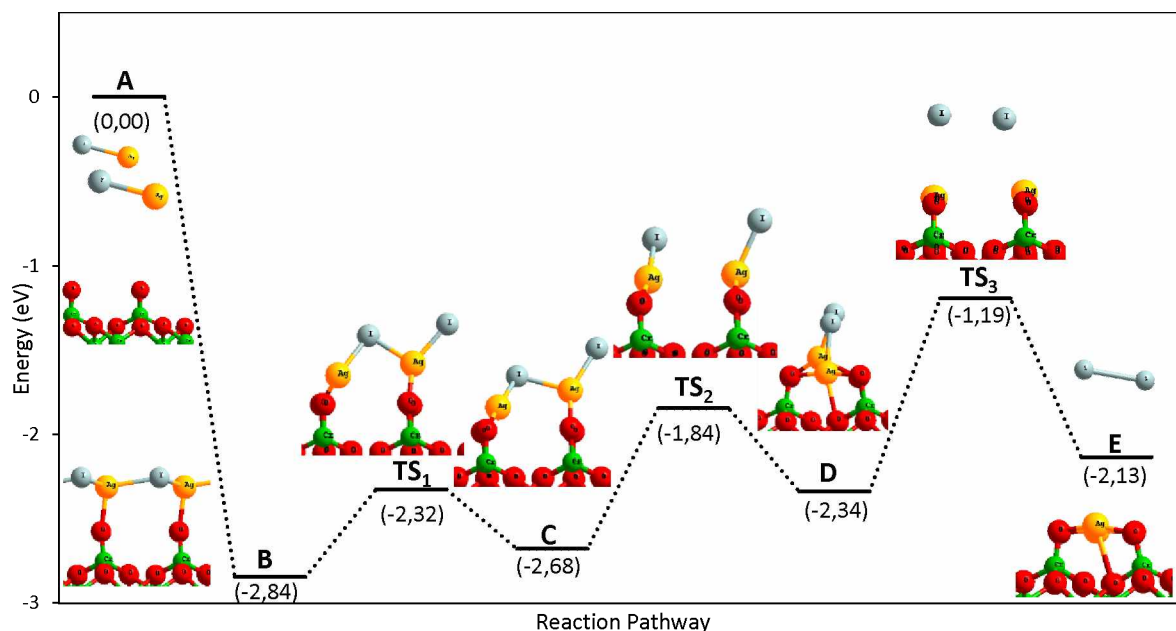


**Figure 7.** Energy diagram for formation of  $I_2$  on Chromyl surface covered by 50% of AgI. Chromium: green. Oxygen: red. Silver: yellow. Iodine: grey.

At a 100% AgI coverage on a chromyl surface, the formation of  $I_{2(g)}$  is almost unlikely. It occurs only within a very small range of temperature (569-613 K). Since, at this coverage, chains and rings are formed on the surfaces at this coverage, we can expect that the activation energy will be equivalent to or higher than that at a 50% coverage. Many possible reaction pathways may occur, such as the formation of  $I_2$  and (simultaneously) or AgI, since the thermodynamic calculations show that the desorption is less likely on the fully covered surfaces, these mechanisms are not studied.

The formation of  $I_2(g)$  is impossible on the  $Cr_2O_3Cr$  and  $Fe_2O_3Fe$  surfaces under normal condition. The sublimation of  $AgI(g)$  on these two surfaces is more favourable. From a thermodynamic point of view, the formation of  $I_{2(g)}$  should be occurring on the chromyl surface. Kinetics shows that the  $I_{2(g)}$  formation will be faster at low surface coverage.

### 3.2.2. Formation of $I_{2(g)}$ on oxide surfaces with $CdI_2$ adsorbed.

The insertion of thermodynamic correction terms to  $I_{2(g)}$  and  $CdI_{2(g)}$  at different temperatures permits to calculate the Gibbs free energies of the of  $I_{2(g)}$  formation and  $CdI_{2(g)}$  sublimation on three most interested surfaces ( $Cr_2O_3Cr$ , Chromyl,  $Fe_2O_3Fe$ ) as functions of temperature. The results are presented in **Figure 8**.

It can be noticed that the formation of  $I_{2(g)}$  is not possible on the  $Cr_2O_3Cr$  and  $Fe_2O_3Fe$  surface since the sublimation of  $CdI_{2(g)}$  occurs at lower temperatures (**Figure 8a and c**). On  $Cr_2O_3Cr$  surfaces the temperatures needed for the sublimation of  $CdI_{2(g)}$  at 25 % and 50 % coverages are almost the same (about 460 K). On the  $Fe_2O_3Fe$  surface, these temperatures are higher (760 K and 710 K at 25% and 50% resp.). Since  $CdI_2$  molecules from a 2D network that does not form strong bonds with the surface at a 100% coverage, the desorption could occur at a very low temperature (190 K on the  $Cr_2O_3Cr$  surface and 235 K on the  $Fe_2O_3Fe$  surface). **Figure 8b** shows the Gibbs free energies of the  $I_{2(g)}$  formation and the sublimation of  $CdI_{2(g)}$  on a chromyl surface. At a 25% coverage, the formation of  $I_{2(g)}$  is thermodynamically favoured, however, at about 640 K, the sublimation of  $CdI_{2(g)}$  becomes more favourable. At a 50 % coverage and at low temperature, the formation of  $I_{2(g)}$  is more favourable than the  $CdI_2$  sublimation, but the  $I_{2(g)}$  formation Gibbs free energy is positive, the partial pressure of the gas remains low. Above 295 K, the Gibbs free energy becomes negative and the sublimation of  $CdI_{2(g)}$  (red slashed line) is more favourable than the formation of  $I_{2(g)}$ . On a surface totally covered by  $CdI_2$ , the sublimation of  $CdI_{2(g)}$  (red dotted line) is always favourable and at 205 K the reaction becomes possible.

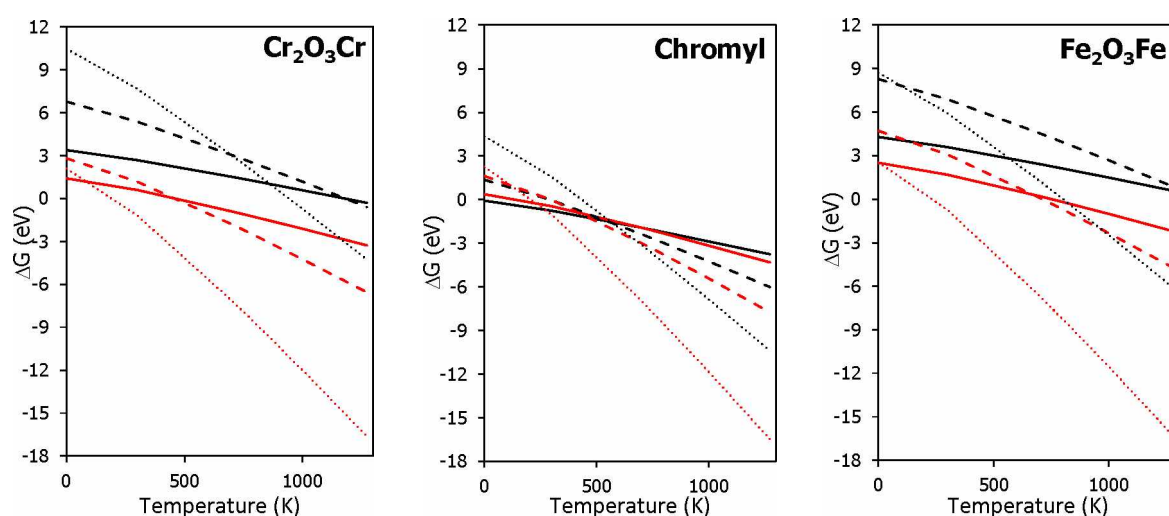


**Figure 8.** Gibbs free energy for the formation of  $I_{2(g)}$  (black lines) and sublimation (red lines) of  $CdI_{2(g)}$  on three surfaces ( $Cr_2O_3Cr$ , Chromyl,  $Fe_2O_3Fe$ ) for  $AgI$  coverages equal to 25% (plain line) 50% (dashed line) and 100 % (dotted line) in function of the temperature varying from 0 to 1273 K.

Since the formation of  $I_{2(g)}$  on the chromyl surface is possible at a 25%  $CdI_2$  coverage, the reaction pathway is discussed. First,  $CdI_2$  is adsorbed on the top position of the terminal oxygen atom (**Figure 9, A**  $\rightarrow$  **B**,  $\Delta E = -0.09$  eV). Then,  $CdI_2$  moves to a position between two terminal oxygen atoms and forms two Cd-O bonds (**B**  $\rightarrow$  **C**). Finally, the distance between two iodine atoms decreases until becoming similar to that of the iodine gas ( $I_{2(g)}$ ,  $d_{I-I, th} = 2.66$  Å, **C**  $\rightarrow$  **D**),

which leads to the release of  $I_{2(g)}$  from the surface. It can be noticed that all these steps are exothermic. In step  $B \rightarrow C$ , the  $CdI_2$  molecule moves towards two terminal oxygen atoms ( $B \rightarrow TS_1$ ) and forms a tetrahedral structure with cadmium atom in the centre of two iodine atoms and two terminal oxygen atoms ( $C$ ). The activation energy of this step is quite small (0.06 eV), hence the equilibrium between  $B$  and  $C$  is reached at all temperatures. In the step  $C \rightarrow D$ , the distance between two iodine atoms decreases to reach the bond length in the  $I_{2(g)}$  molecule ( $C$ : 3.37 Å;  $TS_2$ : 2.97 Å and  $D$ : 2.66 Å). The activation energy of this step is slightly higher than that of  $B \rightarrow C$  (0.17 eV). We can conclude that the decomposition of  $CdI_2$  on an oxidized surface is very fast and prevents the formation of an important coverage.  $CdI_2$  is a very probable source of gaseous iodine.

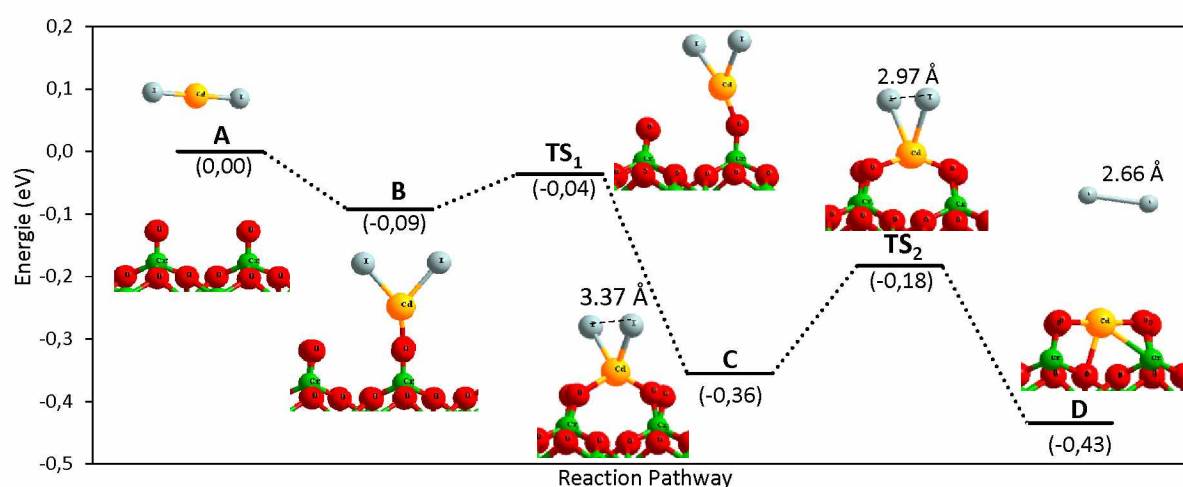


**Figure 9.** Energy diagrams of the  $I_2$  formation at a 25%  $CdI_2$  on the chromyl surface. Chromium: green. Oxygen: red. Cadmium: yellow. Iodine: grey.

In conclusion, when  $CdI_2$  is adsorbed on the  $Cr_2O_3Cr$  and  $Fe_2O_3Fe$  surfaces the formation of  $I_{2(g)}$  is impossible, Whereas the sublimation of  $CdI_2$  is probable. This result is similar to the conclusion on  $AgI$  adsorption studies. The formation of  $I_{2(g)}$  occurs only at a 25 %  $CdI_2$  coverage on the chromyl surface at temperatures lower than 640 K, at higher temperatures, sublimation starts.

### 3.2.3. Formation of $I_{2(g)}$ on oxide surfaces with an oxidant.

**Figure 5** and **Figure 8**, show that the formation of  $I_{2(g)}$  on  $Cr_2O_3Cr$  and  $Fe_2O_3Fe$  surfaces is impossible. As a result, the formation of  $I_{2(g)}$  on these two surfaces necessitates the addition of an oxidant. In nuclear studies,  $OH^\bullet$  is often used as an oxidant since the hydroxyl radical is produced by water radiolysis. The energies of these reactions are grouped in **Table 6**. It can be

observed that, once the oxidant is added, the formation of  $I_2$  is observed spontaneously (exothermic reaction).

**Table 6.**  $I_{2(g)}$  formation energy on chromium oxide and iron oxide surfaces in presence of an oxidant ( $OH^\bullet$ ).

Reaction	Model	$\Delta$ Energy (eV)
Surface-2AgI + $2OH^\bullet \rightarrow$ Surface-2AgI-2OH $\rightarrow$	$Cr_2O_3Cr$	-2.84
Surface-2Ag-2OH $^\bullet$ + $I_2(g)$	$Fe_2O_3Fe$	-3.29
Surface-CdI $_2$ + $2OH^\bullet \rightarrow$ Surface-CdI $_2$ -2OH $\rightarrow$	$Cr_2O_3Cr$	-3.40
Surface-Cd-2OH $^\bullet$ + $I_2(g)$	$Fe_2O_3Fe$	-3.24

#### 4. Conclusion

In our paper, we study the adsorption of control rod metal iodides on the oxide surfaces (chromium oxides and iron oxides) that constitute the outer surfaces of the RCS. The molecular adsorption is generally more favourable than the dissociative one on almost all these surfaces (except for AgI on the chromyl surface at a coverage lower than 25%).

When AgI is adsorbed onto these surfaces, and the coverage increases, AgI forms chains or 2D networks on the surface with bonds between silver atoms and oxygen atoms from the surface. The silver atom is located in a threefold hollow site on all the surfaces except the chromyl one (oxidized chromium oxide surface).

When  $CdI_2$  is adsorbed molecularly on these surfaces, only Cd forms bonds with oxygen atoms of the surface. Cd forms three bonds with the surface oxygen atoms on most of the surfaces except the chromyl surface (oxidized chromium oxide). At high coverage, it forms a 2D network that has no direct interaction with the surface and is sublimated at low temperature. The adsorption of these two metallic iodides is always more favourable on a neutral surface than on a modified surface (oxidized or hydrated). The adsorption on the chromium oxide surface is always less favourable than on iron oxide surface.

H. Hijazi[19] has found that the formation of  $I_{2(g)}$  from AgI aerosols by gas process without an oxidant is impossible. However, in our case, it is possible to form  $I_{2(g)}$  from AgI adsorbed on an already oxidized chromium oxide surface (Chromyl). At low coverages the formation is easier than at higher ones, which induce the formation of strong bonds between AgI moieties.

This conclusion can explain the partial re-vaporization of  $I_{2(g)}$  on stainless steel surface observed in experimental work[21].

The formation of  $I_{2(g)}$  from  $CdI_2$  adsorbed on the RCS surfaces is similar to the formation from  $AgI$ . The formation of  $I_{2(g)}$  occurs rapidly on the oxidized surface when the coverage is low.

For both systems, the formation of  $I_{2(g)}$  is unfavourable on a neutral surfaces ( $Cr_2O_3Cr$  and  $Fe_2O_3Fe$ ), except under the presence of an oxidant such as  $OH^\bullet$ .

## Acknowledgements

This work has been supported by the Ministry of Higher Education Research and Innovation under the program Investissements d’Avenir MiRE managed by the ANR (ANR-11-RSNR-0013-01).

## Reference

- [1] G. Ducros, P.P. Malgouyres, M. Kissane, D. Boulaud, M. Durin, Fission product release under severe accidental conditions: General presentation of the program and synthesis of VERCORS 1-6 results, *Nucl. Eng. Des.* 208 (2001) 191–203. doi:10.1016/S0029-5493(01)00376-4.
- [2] V. Preedy, G. Burrow, R. Watson, *Comprehensive Handbook of Iodine*, Elsevier, 2009. doi:10.1016/B978-0-12-374135-6.X0001-5.
- [3] Nuclear Energy Agency/ Committee on the Safety of Nuclear installations, *Insights into the control of the release of iodine, cesium, strontium and other fission products in the containment by severe accident management*, (2000).
- [4] Nuclear Regulatory Commission, *Reactor safety study. An assessment of accident risks in US commercial nuclear power plants. Executive summary: main report*, Nuclear Regulatory Commission, 1975.
- [5] C.F. Weber, E.C. Beahm, T.S. Kress, *Models of iodine behavior in reactor containments*, Oak Ridge, TN, 1992. doi:10.2172/6982565.
- [6] C.-C. Lin, Chemical effects of gamma radiation on iodine in aqueous solutions, *J. Inorg. Nucl. Chem.* 42 (1980) 1101–1107. doi:10.1016/0022-1902(80)80417-9.
- [7] J.W. Yeon, S.H. Jung, Effects of temperature and solution composition on evaporation of iodine as a part of estimating volatility of iodine under gamma irradiation, *Nucl. Eng.*

- Technol. 49 (2017) 1689–1695. doi:10.1016/j.net.2017.07.018.
- [8] D.A. Petti, Silver-indium-cadmium control rod behavior in severe reactor accidents, Nucl. Technol. 84 (1989) 128–151.
- [9] M. Furrer, T. Gloor, Einfluss von metallischem Silber und Sauerstoff auf die Radiolyse von Cäsiumiodidlösungen, Eidgenössisches Institut für Reaktorforschung, 1987.
- [10] M. Furrer, R.C. Cripps, E. Frick, Iodine severe accident behaviour code IMPAIR 2, (1989).
- [11] J. Sugimoto, M. Kajimoto, K. Hashimoto, K. Soda, Short overview on the definitions and significance of the late phase fission product aerosol/vapour source, (1994).
- [12] P.D.W. Bottomley, K. Knebel, S. Van Winckel, T. Haste, S.M.O. Souvi, A. Auvinen, et al., Revaporisation of fission product deposits in the primary circuit and its impact on accident source term, Ann. Nucl. Energy. 74 (2014) 208–223. doi:10.1016/j.anucene.2014.05.011.
- [13] J. Kalilainen, T. Kärkelä, R. Zilliacus, U. Tapper, A. Auvinen, J. Jokiniemi, Chemical reactions of fission product deposits and iodine transport in primary circuit conditions, Nucl. Eng. Des. 267 (2014) 140–147. doi:10.1016/j.nucengdes.2013.11.078.
- [14] D. Obada, A.S. Mamede, N. Nuns, A.C. Grégoire, L. Gasnot, Combined ToF-SIMS and XPS characterization of 304L surface after interaction with caesium iodide under PWR severe accident conditions, Appl. Surf. Sci. 459 (2018) 23–31. doi:10.1016/j.apsusc.2018.07.212.
- [15] T. Haste, F. Payot, P.D.W. Bottomley, Transport and deposition in the Phébus FP circuit, Ann. Nucl. Energy. 61 (2013) 102–121. doi:10.1016/j.anucene.2012.10.032.
- [16] T.S. Kress, E.C. Beahm, C.F. Weber, G.W. Parker, Fission Product Transport Behavior, Nucl. Technol. 101 (1993) 262–269. doi:10.13182/NT93-A34789.
- [17] L. Cantrel, T. Albiol, L. Bosland, J. Colombani, F. Cousin, A.-C. Grégoire, et al., Research Works on Iodine and Ruthenium Behavior in Severe Accident Conditions, J. Nucl. Eng. Radiat. Sci. 4 (2018) 020903. doi:10.1115/1.4038223.
- [18] L. Bosland, L. Cantrel, Iodine behaviour in the circuit and containment: modeling improvements in the last decade and remaining uncertainties, in: Proc. Int. OECD-NEA/NUGENIA-SARNET, Marseille, France, 2015.

- [19] H. Hijazi, Réactivité chimique des aérosols d'iode en conditions accidentelles dans un réacteur nucléaire, Université de Lille 1, 2017.
- [20] D. Obada, L. Gasnot, A.-S. Mamede, A.-C. Grégoire, Assessment of medium-term radioactive releases in case of a severe nuclear accident on a pressurized water reactor: Experimental study of fission products re-vaporisation from deposits (Cs, I), in: 2017 Int. Congr. Adv. Nucl. Power Plants, ICAPP 2017 - A New Paradig. Nucl. Power Safety, Proc., 2017.
- [21] D. Obada, Evaluation de rejets moyen-terme en situation accidentelle grave d'un réacteur à eau pressurisée : étude expérimentale de la re-vaporisation de dépôts de produits de fission (Cs, I), PhD University of Lille, 04 december 2017, n.d.
- [22] A.-C. Grégoire, T. Haste, Material release from the bundle in Phébus FP, *Ann. Nucl. Energy*. 61 (2013) 63–74. doi:10.1016/j.anucene.2013.02.037.
- [23] N. Girault, L. Bosland, J. Dienstbier, R. Dubourg, C. Fiche, LWR Severe Accident simulation: Fission Product behavior in FPT2 experiment, *Nucl. Technol.* 169 (2010) 218–238. doi:<https://doi.org/10.13182/NT10-A9375>.
- [24] M. Gouëlle, J. Kalilainen, P. Rantanen, T. Kärkelä, A. Auvinen, Experimental Study of the Cadmium Effects on Iodine Transport in the Primary Circuit During Severe Nuclear Accident, in: Vol. 3 Next Gener. React. Adv. React. Nucl. Saf. Secur., ASME, 2014. doi:10.1115/ICONE22-31042.
- [25] A.-C. Grégoire, S. Morin, L. Cantrel, Main Outcomes of the IRSN experimental ISTP-CHIP and CHIP+ Programs, in: 27th Int. Conf. Nucl. Energy New Eur. Sept. 10-13, 2018, Portoroz, Slovenia, n.d.
- [26] A. Mamede, N. Nuns, A. Cristol, L. Cantrel, S. Souvi, S. Cristol, Applied Surface Science Multitechnique characterisation of 304L surface states oxidised at high temperature in steam and air atmospheres, *Appl. Surf. Sci.* 369 (2016) 510–519. doi:<http://dx.doi.org/10.1016/j.apsusc.2016.01.185>.
- [27] S.M.O. Souvi, M. Badawi, F. Virot, S. Cristol, L. Cantrel, J.-F. Paul, Influence of water, dihydrogen and dioxygen on the stability of the Cr<sub>2</sub>O<sub>3</sub> surface: A first-principles investigation, *Surf. Sci.* 666 (2017) 44–52. doi:10.1016/j.susc.2017.08.005.
- [28] S.M.O. Souvi, M. Badawi, J.-F. Paul, S. Cristol, L. Cantrel, A DFT study of the hematite surface state in the presence of H<sub>2</sub>, H<sub>2</sub>O and O<sub>2</sub>, *Surf. Sci.* 610 (2013) 7–15.

doi:10.1016/j.susc.2012.12.012.

- [29] J.P. Perdew, K. Burke, M. Ernzerhof, Generalized Gradient Approximation Made Simple, *Phys. Rev. Lett.* 77 (1996) 3865–3868. doi:10.1103/PhysRevLett.77.3865.
- [30] G. Kresse, J. Furthmüller, Efficiency of ab-initio total energy calculations for metals and semiconductors using a plane-wave basis set, *Comput. Mater. Sci.* 6 (1996) 15–50. doi:10.1016/0927-0256(96)00008-0.
- [31] G. Kresse, J. Hafner, *Ab initio* molecular-dynamics simulation of the liquid-metal–amorphous-semiconductor transition in germanium, *Phys. Rev. B.* 49 (1994) 14251–14269. doi:10.1103/PhysRevB.49.14251.
- [32] W. Kohn, L.J. Sham, Self-consistent equations including exchange and correlation effects, *Phys. Rev.* 140 (1965) A1133–A1138. doi:10.1103/PhysRev.140.A1133.
- [33] G. Kresse, D. Joubert, From ultrasoft pseudopotentials to the projector augmented-wave method, *Phys. Rev. B.* 59 (1999) 1758–1775. doi:10.1103/PhysRevB.59.1758.
- [34] G. Rollmann, A. Rohrbach, P. Entel, J. Hafner, First-principles calculation of the structure and magnetic phases of hematite, *Phys. Rev. B.* 69 (2004) 165107. doi:10.1103/PhysRevB.69.165107.
- [35] A. Rohrbach, J. Hafner, G. Kresse, *Ab initio* study of the (0001) surfaces of hematite and chromia: Influence of strong electronic correlations, *Phys. Rev. B.* 70 (2004) 125426. doi:10.1103/PhysRevB.70.125426.
- [36] D. Sheppard, R. Terrell, G. Henkelman, Optimization methods for finding minimum energy paths, *J. Chem. Phys.* 128 (2008). doi:10.1063/1.2841941.
- [37] G. Henkelman, B.P. Uberuaga, H. Jónsson, Climbing image nudged elastic band method for finding saddle points and minimum energy paths, *J. Chem. Phys.* 113 (2000) 9901–9904. doi:10.1063/1.1329672.
- [38] G. Henkelman, H. Jónsson, Improved tangent estimate in the nudged elastic band method for finding minimum energy paths and saddle points, *J. Chem. Phys.* 113 (2000) 9978–9985. doi:10.1063/1.1323224.
- [39] D. Ruelle, *Thermodynamic Formalism-The Mathematical Structures of Equilibrium Statistical Mechanics*, Second Edi, CAMBRIDGE UNIVERSITY PRESS, 2004.

